PCCP

PAPER

Adsorption of NGF and BDNF derived peptides on gold surfaces†

Cite this: *Phys. Chem. Chem. Phys.*, 2014, **16**, 1536

Giuseppe Forte,[a] Alessio Travaglia,[b] Antonio Magrì,[c] Cristina Satriano*[d] and Diego La Mendola*[e]

Received 16th June 2013,
Accepted 14th November 2013

DOI: 10.1039/c3cp52499j

www.rsc.org/pccp

This study tackles the interaction between gold surfaces and two peptide fragments named NGF(1-14) and BDNF(1-12), able to mimic the proliferative activity of the nerve growth factor (NGF) and the brain derived neurotrophic factor (BDNF), respectively. The physical adsorption processes on the solid surface from both single and binary peptide solutions, at physiological and acid pH, were investigated by QCM-D and CD experiments, as well as by molecular dynamics calculations. The relevant physicochemical properties at the hybrid bio-interface, including peptide–surface interaction, conformational changes, hydrodynamic thickness, viscoelastic parameters, and competitive *vs.* synergic behaviour of the two peptide fragments towards the surface, were scrutinized. Biological assays with neuronal cells pointed to the maintenance of the biological activity of NGF(1-14) and BDNF(1-12) peptide molecules within the adlayers on the gold surface.

1. Introduction

Gold is extensively used as substrate material for functionalization with biomolecules, such as gold nanoparticles, which show great promise as therapeutic delivery vectors and intracellular imaging agents.[1]

The immobilization of biomolecules on the solid surface might be achieved through either covalent or non-specific physisorption driven by electrostatic/hydrophobic interactions.[2] The latter approach offers several advantages, in terms of easy maintenance of conformational degrees of freedom, reversible interaction with the surface, and enhanced stability for the selective cell and nuclear targeting.[3–6] Indeed, the last point remains a significant practical challenge in the use of nanoparticles *in vivo*.

We describe herein a physicochemical investigation of the interaction between gold oxide surfaces and two peptides, NGF(1-14) and BDNF(1-12), designed and synthesized according to a peptide-mimetic strategy for the nerve growth factor (NGF) and the brain-derived neurotrophic factor (BDNF), respectively.[7,8] These two proteins represent the most important neurotrophic factors of the family of neurotrophins (NTs), of outstanding importance, because of their widespread expression in nearly all neuronal populations and having a well-known physiological role in neuronal survival, process outgrowth and regulation of synaptic plasticity. In particular, NGF and BDNF are the most abundant NTs, often residing in the hippocampal region of the brain.[9–11] Moreover, they have recently gained great interest as therapeutic agents for neurological pathologies, including schizophrenia and Alzheimer's disease.[12]

The N-terminal domains of these proteins play a crucial role in the selective binding and the activation of TrkA and TrkB, the respective receptors involved in triggering pro-survival signals.[13] Accordingly, NGF(1-14) and BDNF(1-12) peptides, encompassing the N-terminal sequences, respectively, of NGF and BDNF, have been reported to induce a cellular proliferation comparable to that found by using the respective whole proteins.[7,8]

Such a mimicking ability of NGF- and BDNF-derived peptides suggests their potential use as drugs to overcome the pharmacological limits of the corresponding proteins, including the activation of the p75 receptor and its downstream pro-apoptotic signals, and the painful administration.[14]

In the present study we address the immobilization of NGF(1-14) and BDNF(1-12) peptides on gold surfaces, achieved by physical adsorption from single peptide solution as well as under competitive/synergic conditions from the binary

[a] *Department of Pharmaceutical Sciences, University of Catania, Viale Andrea Doria, 6, I-95125, Italy*
[b] *Centre for Neural Science, New York University, Washington Place, 4, New York, NY 10003, USA*
[c] *Institute of Biostructures and Bioimages – Catania, National Council of Research (CNR), Viale Andrea Doria, 6, I-95125, Catania, Italy*
[d] *Department of Chemical Sciences, University of Catania, Viale Andrea Doria, 6, I-95125 Catania, Italy. E-mail: csatriano@unict.it; Fax: +39 095 580138; Tel: +39 095 7385136*
[e] *Department of Pharmacy, University of Pisa, via Bonanno Pisano, 6, I-56100 Pisa, Italy. E-mail: lamendola@farm.unipi.it*

† Electronic supplementary information (ESI) available: S1: lengthy experimental details; S2: chemical and topographical characterization of the gold substrates. See DOI: 10.1039/c3cp52499j

equimolecular solution. A combined approach of experimental investigations, by means of quartz crystal microbalance with dissipation monitoring (QCM-D) and circular dichroism (CD), and theoretical calculations, by molecular dynamics (MD), was used to compare the peptide–solid surface interaction at the physiological pH and at the acid pH of 5.5, taken as a model microenvironment for pathological conditions, including hypoxia, ischemia and cancer.[15,16]

Preliminary biological assays with neuroblastoma SH-SY5Y cells were performed to assess whether the activity exhibited by the NGF(1-14) and BDNF(1-12) free peptides in the solution[7,8] was maintained after the immobilization as adlayers of different hydrodynamic thickness and viscoelastic character at the gold surfaces.

2. Experimental methods

2.1 Peptide synthesis and purification

NGF(1-14) and BDNF(1-12) peptide sequences (see Chart 1) were synthesized by a solid-phase-peptide-synthesis (SPPS) strategy on a Pioneer Peptide Synthesizer. Both peptides were prepared using the amidated C-terminal. All amino acid residues were added according to the TBTU/HOBT/DIEA activation protocol for Fmoc chemistry on a NovaSyn-TGR resin (loading 0.18 mmol g^{-1}; resin 1 g, 0.33 mmol scale synthesis). Other experimental details have already been reported.[6–8]

Peptides were purified by means of preparative reverse-phase high-performance liquid chromatography (rp-HPLC), using a Varian PrepStar 200 model SD-1 chromatography system equipped with a Prostar photodiode array detector with detection at λ = 222 nm. The peptide characterization was carried out by analytical rp-HPLC and ESI-MS.[7,8] For NGF(1-14) (SSSHPIFHRGEFSV-NH_2, $C_{71}H_{103}N_{22}O_{20}$): calculated mass = 1584.73, ESI-MS [observed m/z: $(M + H)^+$ 1586.7; $(M + 2H)^{2+}$ 793.7]. For BDNF(1-12) (HSDPARRGELSV-NH_2, $C_{54}H_{91}N_{21}O_{18}$): calculated mass = 1322.4, ESI-MS [observed m/z: $(M + H)^+$ 1323.2; $(M + 2H)^{2+}$ 662.1].

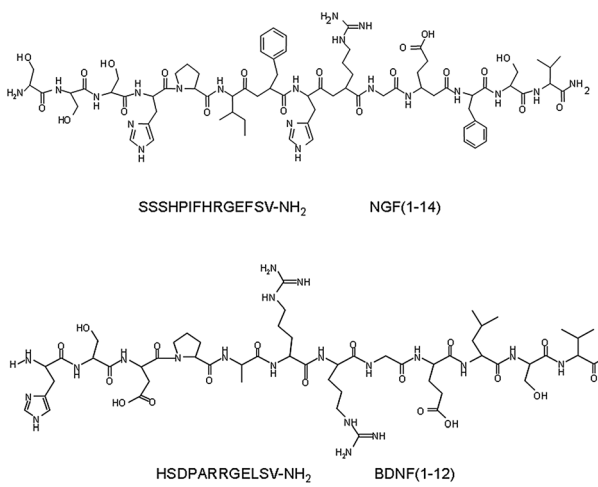

Chart 1 Schematic representation of NGF(1-14) and BDNF(1-12) primary sequences.

2.2 Gold substrate preparation and physicochemical characterization

Peptide adsorption experiments were run on gold-coated 5.0 MHz AT-cut quartz resonators (Biolin Scientific, Finland) as the adsorbent surface. The sensor crystals were cleaned by 10 minutes treatment in base piranha solution ($H_2O : NH_3 : H_2O_2$, 5 : 1 : 1 at 75 °C), followed by copious rinsing with Millipore water, and argon blow drying. Prior to the experiments, the gold substrates were treated with UV ozone for 15 minutes, rinsed with Millipore water, argon blow dried and immediately mounted on the QCM-D measurement cell.

The surface characterization of the used substrates was carried out by X-ray photoelectron spectroscopy (XPS), atomic force microscopy (AFM), and static water contact angle (WCA) measurements with the use of a three-liquid technique (tricresyl phosphate, pure deionized water, and glycerol) for determination of polar acid–base (AB) and dispersive Lifshitz van der Waals (LW) components of surface free energy.[17,18]

2.3 QCM-D measurements

QCM-D measurements were carried out on a Q-Sense E1 unit (Biolin Scientific, Finland) running under QSoft401 software in flow mode (50 μL min^{-1}). The working principle of QCM-D relates to the piezoelectric response of a AT-cut quartz sensor that, by application of an AC voltage with a frequency close to the crystal resonant frequency (f_0), is excited to a purely shear mode of oscillation. The frequency change (Δf) is related to the hydrated mass adsorbed on the surface, according to the linear Sauerbrey's relationship:[19]

$$\Delta m = (C/n)\,\Delta f \quad (1)$$

where Δm is the mass adsorbed and n is the harmonic number and

$$C = (t_q \rho_q)/f_0 \quad (2)$$

with t_q and ρ_q being, respectively, the thickness and the density of quartz, and C, the sensitivity constant, is ~ -17.7 Hz ng cm^{-2} for a 5-MHz crystal. The Sauerbrey equation only holds true for thin, light (relative to the electrode mass), homogenously distributed and rigid, firmly adsorbed, film onto the electrode surfaces that couple to the electrode's oscillation.

The other parameter monitored in QCM-D is the dissipation (D) factor, measuring the amplitude damping of the crystal vibration after the alternating electric field has been turned off, and defined as:

$$D = E_{diss}/(2\pi \cdot E_{stored}) \quad (3)$$

where E_{diss} is the energy dissipated during one oscillation period and E_{stored} is the energy stored during oscillation.[20] The dissipation for a typical crystal is on the order of 10^{-6}.

The fundamental, along with the third, fifth, seventh and ninth harmonics of the fundamental frequency were monitored (n = 3–9); frequency shifts were normalized by dividing by the overtone number.

Peptide adsorption experiments were run at 298 K in phosphate buffer saline (PBS) solution (0.01 M phosphate buffer, 0.0027 M potassium chloride and 0.137 M sodium chloride, pH = 7.4 at 298 K, Sigma Aldrich). The PBS buffer was acidified with HCl to the pH of 5.5 (at 298 K). Peptide solutions were prepared at the final concentration of 6×10^{-4} M for each peptide. The binary peptide solutions were prepared in a 1 : 1 molar ratio.

2.3.1 Data analysis. Plots of frequency *versus* dissipation (D–f) were generated by using the third overtone. This kind of plot, by eliminating time as the explicit variable, allows visualizing the faster or slower kinetic steps simply as denser or scattered data points, respectively. Moreover, the curve slope change is a marker of the transition between different kinetic phases.[21] Data analysis was performed using Q-Tools3 software from Q-Sense.

To account for the viscoelastic properties of the adsorbed layer, the Δf and ΔD values at multiple overtones were modeled according to the Voigt viscoelastic model provided with the software that, in turn, generates information regarding the thickness, shear and viscosity of the attached layer.

In such a model, according to the mechanical element analogy for a viscoelastic system consisting of a spring and a dashpot, the spring corresponds to the shear rigidity and the dashpot to the viscosity; the retardation time is defined as their ratio. The governing viscoelastic functions for the Voigt element are defined using these three variables.[22]

2.4 CD measurements

CD spectra were obtained at 298 K under a constant flow of N_2 on a Jasco model 810 spectropolarimeter, at a scan rate of 50 nm min^{-1} and a resolution of 0.2 nm. The path length was 1 cm. The spectra were recorded as an average of 20 scans. Calibration of the instrument was performed with a 0.06% solution of ammonium camphorsulfonate in water.

All the solutions were freshly prepared using double distilled water. The CD spectra were acquired in the 190–400 nm wavelength region by using peptide concentrations ranging from 5.0×10^{-6} M to 1.0×10^{-5} M in ultrapure water.

2.5 Cellular experiments

Human neuroblastoma SH-SY5Y cells (purchased from ATCC) were grown in DMEM-F-12 (1 : 1) medium, supplemented with 10% fetal bovine serum, 1% penicillin/streptomycin, 2 mM l-glutamine and maintained in a humidified incubator at 310 K in 5% CO_2. Gold substrates were pre-coated with adlayers of NGF(1-14), BDNF(1-12) or with the mixture of both peptides, following the same incubation times scrutinized in the QCM-D experiments. After incubation and rinsing of samples, cells were plated on them at a density of 1×10^5 in DMEM-F12 medium with 5% fetal bovine serum. The measurements of neuronal survival were assessed 48 hours after plating by 3-(4,5-dimethylthiazol-2-yl)-2,5-diphenyl tetrazolium bromide (MTT) reduction assay. The statistical data significance from experiments conducted in triplicate was assessed by the one-way ANOVA test followed by the Newman–Keuls post-hoc test.

3. Computational methods

Simulations were performed at the molecular mechanics level of approximations by using the Discover package, included in Material Studio (MS) software, and the Consistence Valence Force Field (CVFF) parametrization[23] combined with the CVFF flexible water potential.[24]

In the geometry optimization, using the Smart Minimizer algorithm, a minimization energy procedure was performed starting from an initial structure. During the simulations, Periodic Boundary Conditions (PBC), using the Ewald summation method with a dielectric constant equal to 1, was applied and the electric neutrality condition maintained using Na^+ and Cl^- as counterions. Molecular Dynamics simulations were run under NVT conditions at 298 K (Berendsen thermostat[25] was used with a decay constant of 1 ps) with a 1 fs time step.

The detailed description of the equilibration procedure applied for each configuration (*i.e.*, NGF(1-14)–NGF(1-14), BDNF(1-12)–BDNF(1-12), NGF(1-14)–BDNF(1-12), NGF(1-14)–Au_2O_3 and BDNF-(1-12)–Au_2O_3) is reported in the ESI.†

The system equilibration evidence was provided by the Radial Distribution Function (RDF) and potential energy fluctuation analyses; the simulation was continued for 400 ns. During this time, 20 structures were randomly sampled, for each configuration, and optimized. The structure corresponding to the lowest energy value was considered for the analysis reported in the next section. The orthorhombic *Fdd*2 structure of Au_2O_3 was built by using the data reported by Jones *et al.*,[26] the unit cell was replicated $3 \times 3 \times 3$ along the *a b c* directions. The supercell obtained was cleaved along the 111 plane and the oxygen atoms were saturated with hydrogen. The surface obtained was differently replicated along the plane so that the dimensions of the Au_2O_3 slab, at the end, were $4.85 \times 1.96 \times 12.00$ nm.

To simulate the pH effect, hydrogen atoms in carboxylic residues were replaced with sodium atoms, whilst the NH_2 group in the N-terminal residue of each peptide as well as the guanidinium group of the arginine residues were protonated in all simulations. The imidazole group of histidine was considered protonated only at pH 5.5.

All the calculated energies do not take into account entropic contributions, therefore they are referred to as enthalpies.

4. Results and discussion

4.1 Chemical and topographical characterization of the gold substrates

Contact angle measurements were carried out prior to the peptide adsorption experiments in order to determine the wettability character and surface free energies of the used substrates (see ESI†).

The contact angles decrease after the cleaning procedure and therefore the hydrophilicity of the prepared surfaces is increased compared to that of the untreated ones. In particular, the acid–base polar component of free energy rises over the dispersive Lifshitz-van der Waals one (the AB/LW ratio changes from 0.4 to 0.66), due to the 4.4-fold increase of the Lewis-base component.

This change is related to the removal from the gold surface of contaminative hydrocarbon species and the introduction of electron donor oxygen-containing species, due to the UV ozone treatment (Fig. S1, ESI†).

According to the surface chemical analysis by XPS the chemical structure of the used substrates is consistent with a thin overlayer of Au_2O_3 onto the Au metal sensor substrate.

Moreover, the topography investigation by AFM at the submicron scale (*i.e.*, comparable to the scale length of the 'mean-field' QCM-D technique), indicates a relatively flat topography corresponding to the measured root mean square roughness of about 15 nm (Fig. S2 and S3 in ESI†).

4.2 NGF(1-14) and BDNF(1-12) peptides adsorption on gold: QCM-D

Fig. 1 shows *D*–*f* plots of QCM-D runs of NGF(1-14) and BDNF(1-12) adsorption on the gold surfaces at physiological pH, from single and binary peptide solutions.

In the QCM-D measurements the viscous and elastic contributions of a soft-wet biointerface are taken into account by the simultaneous detection of change in frequency, Δf and dissipation ΔD.

The signal from rigid adlayers is only weakly damped (small $\Delta D/\Delta f$ ratio). Conversely, soft adlayers have a large dissipation factor (high $\Delta D/\Delta f$).

It is interesting to note that, notwithstanding the comparable molecular weights (1584.7 and 1322.4, respectively, for NGF(1-14) and BDNF(1-12)), some similarities in the primary sequence (*e.g.*, in the C-terminus, RGEFSV in NGF(1-14) *vs.* RGELSV in BDNF(1-12), see Chart 1) and close isoelectric points (IEPs) (about 9 for NGF(1-14) and 8 for BDNF(1-12)),[6] the two peptides show huge differences in the interaction with the Au_2O_3. The latter under neutral conditions is expected to bear a negatively charged surface (IEP = 5–6).[27]

In particular, the BDNF(1-12) fragment (blue scatter points), with the largest frequency and dissipation shift values, respectively, of $\Delta f = -10.5 \pm 0.3$ Hz and $\Delta D = 0.4 \pm 0.1$ (10^{-6}), exhibits the highest affinity to bind gold.

The relatively low curve slope indicates a rigid behaviour of the peptide adlayer. In fact, the higher the slope of the *D*–*f* plot, the higher the viscoelastic character of the adlayer.[20–22]

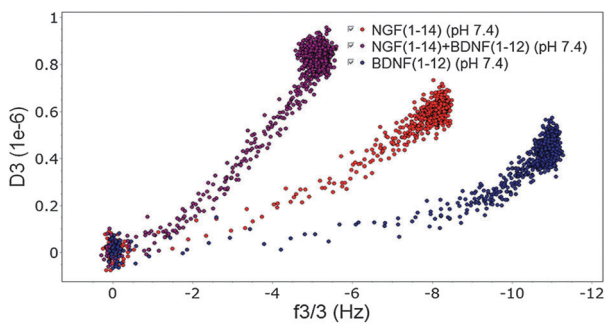

Fig. 1 *D*–*f* plots for adsorption on gold at pH = 7.4 of NGF(1-14) (in red), BDNF(1-12) (in blue) and the equimolar NGF(1-14) + BDNF(1-12) mixture (in purple).

The peptide coverage calculated according to eqn (1) corresponds to an areal mass of about 190 ng cm^{-2}, while the Sauerbrey thickness of the hydrated adlayer is about 1.5 nm.

By taking into account the average molecular dimension of $(3.05 \times 1.66 \times 0.82)$ nm^3 for the BDNF(1-12), such a mass uptake is higher than the ideal coverage for closely packed molecules in a monolayer (ranging from 40 to 160 ng cm^{-2}).

Another important information gained from the *D*–*f* plot is the identification of the various kinetic phases occurring during the adsorption, including hydrodynamic contributions from trapped water and/or conformational rearrangements. Scattered data points are typically found at the beginning of the adsorption process (fast step), whereas overflowing data points correspond to the point when the system reaches the equilibrium, *i.e.*, slower kinetic step(s).[20–22]

The *D*–*f* plot for BDNF(1-12) in Fig. 1 clearly shows an increase of the curve slope at about 95% of the whole Δf shift, therefore pointing to the occurrence of two kinetic phases. Interestingly, such a change corresponds to the fast-to-slow transition of the adsorption process.

These findings can be explained as due to the predominant electrostatic attractive interaction between the oppositely charged BDNF(1-12) molecules and the gold surface, prompting the formation of a stiff adlayer in close contact to the gold surface. According to the primary peptide sequence, the two vicinal arginine (R) residues (see Chart 1) induce a relevant positive charge density, able to trigger the ordered peptide molecules disposition on the negative gold oxide surface.

Moreover, the significant increase of dissipation observed only during the second slower kinetic phase is an indication of extra-adsorption of peptide molecules on the earlier adsorbed ones, as a consequence of strong intermolecular interactions between BDNF (1-12) molecules.

As to the adsorption on the gold surface of NGF(1-14) (red scatter points), the frequency and dissipation shift values, respectively, of $\Delta f = -7.7 \pm 0.4$ Hz and $\Delta D = 0.5 \pm 0.1$ (10^{-6}) suggest a lower level of interaction with the solid surface than BDNF(1-12).

Additionally, the transition from the spread out data points to the narrow-distributed ones (*i.e.*, from the initial fast adsorption to the following slow step) is not accompanied by any significant slope variation, thus there is no indication of any conformational change occurring during the whole adsorption process.

Also, the relatively high $\Delta D/\Delta f$ ratio points to a significant viscoelastic behaviour of the NGF(1-14) adlayer, established already in the early kinetic stages of the adsorption process.

The Sauerbrey approximation of a thin and rigid film is not valid anymore in this case and Voigt modelling must be used. Results give an effective NGF(1-14) adlayer thickness of about 2.2 nm, viscosity of 1.6×10^{-3} kg m^{-1} s^{-1} and shear of 4×10^4 Pa.

According to these values, the calculated Voigt mass is of about 280 ng cm^{-2}, which is higher than the theoretical monolayer coverage (ranging from 45 to 210 ng cm^{-2}) obtained by taking into account the dimensions of $(3.96 \times 1.51 \times 0.84)$ nm^3 for the NGF(1-14) molecule.

Therefore, similarly to the previously described BDNF(1-12), NGF(1-14) also spontaneously adsorbs as multilayer coating on the gold surface. However, the differences in the viscoelastic behaviour as well as in the discernible kinetic phases suggest that a mere electrostatic-driven mechanism cannot be invoked to fully understand the adsorption process, as for the BDNF(1-12) case. For instance, the aromatic rings of the two phenylalanine residues (F, see Chart 1) in the NGF(1-14) sequence, with the consequent local hydrophobic character, might drive different peptide–surface and peptide–peptide molecular interactions at the biointerface with the gold substrate.

Finally, as to the binary peptide mixture (purple scatter points), the *D*–*f* plot in Fig. 1 clearly shows that the biomolecule–gold interface exhibits the highest viscoelastic character. Voigt modelling results in an effective adlayer thickness of about 1.2 nm, a viscosity of 1.5×10^{-3} kg m^{-1} s^{-1} and a shear of 8.0×10^{4} Pa.

The corresponding Voigt mass is of about 150 ng cm^{-2}, thus a lower coverage than the two cases discussed above for single peptide adsorption is obtained. This finding points to a strong interaction between NGF(1-14) and BDNF(1-12) molecules in the bulk solution, in turn decreasing the number of free molecules vicinal to the gold surface able to adsorb onto it.

The results of QCM-D runs at acid pH are shown in Fig. 2. For NGF(1-14) adsorption the *D*–*f* plot does not show any significant change over the curve obtained at physiological pH, both in terms of curve slope and the total frequency and dissipation shifts, which are $\Delta f = -7.2 \pm 0.5$ Hz and $\Delta D = 0.5 \pm 0.1$ (10^{-6}), respectively.

However, the data point dispersion analysis evidences that the transition from the initial fast to the following slower kinetic phases occurs before at acid pH (at about −6 Hz) than at the physiological one (at around −7.5 Hz).

The earlier reaching of the surface saturation point, where the adsorbed peptide molecules start to rearrange and the overall kinetics of the adsorption process slows down, is an indication of different dynamics in the peptide–peptide lateral interaction at the solid surface for the two investigated pH values.

The viscoelastic modelling indicates the reduction in hydrodynamic thickness (Voigt thickness = 1.2 nm), accompanied by the increase of viscous character. In fact, the calculated viscosity and shear values of the NGF(1-14) adlayer formed at acid pH are about 2.5×10^{-3} kg m^{-1} s^{-1} and 3.7×10^{5} Pa, respectively.

In the case of BDNF(1-12) adsorption at the acid pH some differences are evident with respect to the physiological pH.

A significant cut down in the hydrodynamic mass uptake, corresponding to $\Delta f = -5.5 \pm 0.4$ Hz and $\Delta D = 0.3 \pm 0.1(10^{-6})$, is found. On the other hand, analogously to what was found at pH 7.4, the transition from fast to slower kinetic phases parallels that of the conversion from rigid to viscoelastic character of the adlayer.

This fact indicates that, notwithstanding the reduction of peptide mass uptake, the adsorption mechanism for BDNF(1-12) on the gold at the two pH values is similar.

The calculated viscoelastic parameters are of about 1 nm of Voigt thickness, 2.4×10^{-4} kg m^{-1} s^{-1} of viscosity and 1.8×10^{5} Pa of shear.

Finally, the *D*–*f* plot curve for a NGF(1-14) + BDNF(1-12) binary mixture is very similar to that found for BDNF(1-12) alone. This evidence points to a competitive adsorption of the two peptides with a predominant role of BDNF(1-12) in determining the viscoelastic character of the mixed adlayer, in contrast to the synergic adsorption at the neutral pH, where both peptides contributed to the final properties of the mixed adlayer.

Ex-situ XPS analyses of the gold sensors recovered after the *in situ* QCM-D adsorption experiments confirmed the immobilization of irreversibly bound peptide molecules by the detection of the nitrogen signal, which can be taken as a peptide marker (data not shown).

The characterization of the two peptides in the aqueous solution, both alone and in the equimolar mixture, was carried out by means of circular dichroism analyses at the two pH values of interest (Fig. 3).

CD spectra of the NGF(1-14) + BDNF(1-12) 1 : 1 binary solution at a pH of 7.4 show the decrease of the dichroic signal

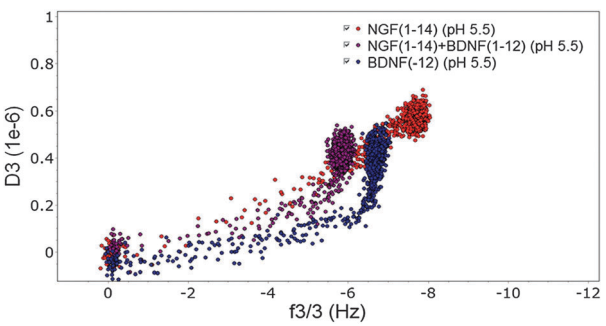

Fig. 2 *D*–*f* plots for adsorption on gold at pH = 5.5 of NGF(1-14) (in red), BDNF(1-12) (in blue) and the equimolar NGF(1-14) + BDNF(1-12) mixture (in purple).

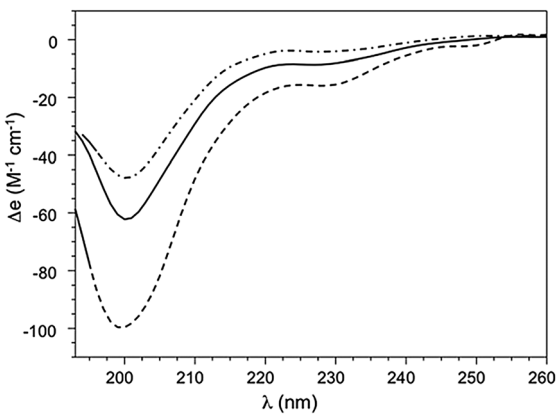

Fig. 3 CD spectra of NGF(1-14) and BDNF(1-12) peptides in aqueous solution. Both the calculated spectrum given by the sum of the experimental single peptide spectra (5×10^{-6} M) and the experimental spectrum of the binary peptide solution (1 : 1 molar ratio, 5×10^{-6} M) are shown. Solid line: calculated spectrum at pH = 7.4. Dashed line: experimental spectrum at pH = 7.4. Dot-dashed line: overlapping experimental and calculated spectra at pH = 5.5.

(see solid line *vs.* dashed line curves), thus indicating a direct interaction between the two peptides. On the other hand, a negligible interaction between NGF(1-14) and BDNF(1-12) molecules at the pH of 5.5 can be deduced by the invariance of the experimental spectrum of the equimolar solution with respect to the sum spectrum (dashed-dot line).

To confirm the peptide interaction (aggregation) in terms of dimerization, experiments at the lower concentration of 1.5×10^{-6} M have been carried out. However, the used concentration is very close to the signal-to-noise detection limit of our experimental setup, the lower concentration spectra being too poor to exhibit the expected differences.

4.3 NGF(1-14) and BDNF(1-12) peptides adsorption on gold: MD results

Geometry optimization in bulk solution gives energy interactions of the homodimers of 21.9 kcal mol^{-1}, for NGF(1-14)–NGF(1-14) and 23.1 kcal mol^{-1}, for BDNF(1-12)–BDNF(1-12), respectively. On the other hand, the higher binding energy of 25.8 kcal mol^{-1} is found for the NGF(1-14)–BDNF(1-12) heterodimer.

Molecular dynamics analysis indicates, for each peptide, the absence of an ordered secondary structure, with random aggregate formation when interaction takes place, and confirms the strong entanglement in the heterodimer.

As to the interaction of a single ligand with the Au_2O_3 surface, the configuration corresponding to the peptide backbone parallel to the surface, henceforth named *side-on* orientation, appears to be the more stable among all the configurations (Fig. 4).

Electrostatic forces (occurring between acidic and basic groups) and H-bonding (due to carbonyl oxygen atoms and both amidic and hydroxyl groups) give the main contribution to the physisorption energy. Further relevant short-range forces, *e.g.* VdW, are involved between aliphatic and aromatic groups.

A preferential orientation of electron donor atoms (carbonylic and carboxylic oxygen), and positive charged groups (guanidine) of the peptide sequence towards the gold surface is found. This points to the presence of both electrophilic and nucleophilic active sites on Au_2O_3, corresponding to positively charged Au atoms and negatively charged oxygen atoms.

Calculated physisorption energy values of *side-on* NGF(1-14)–Au_2O_3 and *side-on* BDNF(1-12)–Au_2O_3 are 16.2 kcal mol^{-1} and 18.5 kcal mol^{-1} respectively.

The slightly higher binding energy value calculated for BDNF-(1-12)–Au_2O_3 can be attributed to the greater abundance of charged groups *e.g.* aspartic, glutamic acids and guanidinium groups of arginine with respect to NGF(1-14).

Finally, all MD simulations denote the presence of, at least, a single water layer, which mediates the interaction between the polypeptide aggregate and the surface.[4] Here most of the water molecules are oriented parallel to the surface, thus explaining the observed viscoelastic behaviour of the adlayers.

To get a deeper understanding about the mechanism of adsorption as well as to evidence, if any, differences in the two examined peptides, MD simulations were performed in terms of the time evolution of distance between the peptide and the gold surface, for single NGF(1-14) and BDNF(1-12) molecules, as well as for the peptide aggregates.

The time evolution of the distance from Au_2O_3 of a single peptide molecule, NGF(1-14) or BDNF(1-12), is shown in Fig. 5. In detail, we have evaluated the distance between the side chain carbon atom of the glutamic residue and the gold surface. We note that in physisorbed systems the conformational flexibility is quite reduced because of the non-bonding interactions. In particular we have chosen a sensible moiety of the peptide – *i.e.*, the carboxylic carbon atom of glutamic residue, which is strongly involved in electrostatic interaction with the surface – to report the distance fluctuations.

The fluctuations of such variable over time indicate, for BDNF(1-12), an average value of 4.56 Å and a range between 4.21 Å and 4.92 Å. On the other hand, slightly greater distances were found for NGF(1-14), confirming the lower physisorption

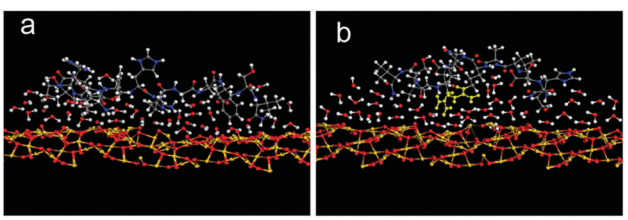

Fig. 4 Relative peptide–surface disposition as obtained by molecular dynamics for NGF(1-14) (a) and BDNF(1-12) (b) at the pH of 7.4. For clarity reasons the water molecules are represented in limited number.

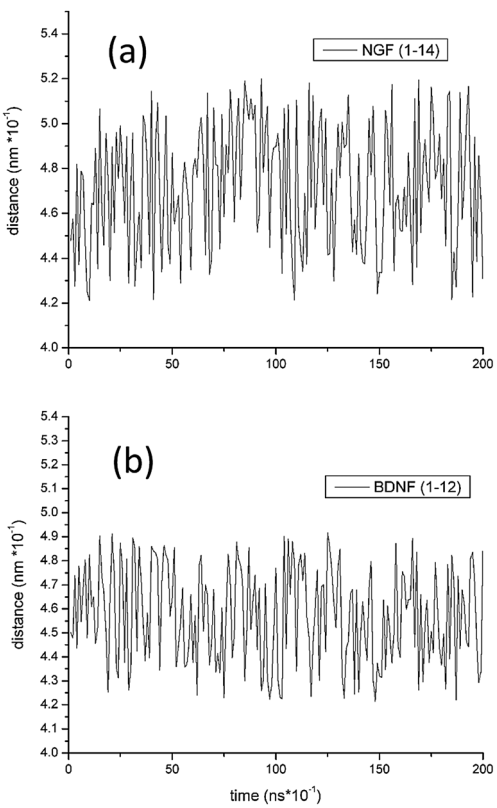

Fig. 5 Fluctuation of the distance over time for: (a) NGF(1-14)–Au_2O_3; (b) BDNF(1-12)–Au_2O_3.

energy value. Protonation of the imidazolic ring, which simulates the effect of a lower pH value, induces, for both NGF(1-14)–Au_2O_3 and BDNF(1-12)–Au_2O_3 interfaces, a negligible change in the average peptide–surface distance with respect to pH 7.4. In fact, as found at physiological pH, the acid groups and protonated basic residues point towards the surface, while the aromatic rings do not affect significantly the binding with Au_2O_3. Consequently, the binding energy values are unchanged.

To get insight into the peptide binding to the surface when adsorbed from a binary mixture *vs.* single peptide solution, we scrutinized the affinity of the entangled polypeptides, both homodimers and heterodimers, with respect to the Au_2O_3 surface (Fig. 6).

During the time evolution the heterodimer–surface distance increases up to about 0.7 nm (Fig. 6c). Analogous trends are found for the homodimer–surface distance evolution for both NGF(1-14) (Fig. 6a) and BDNF(1-12) (Fig. 6b), but a lower slope of the fluctuation curve of the distance *vs.* time is found in comparison with the heterodimer.

Much longer MD simulation could confirm the lower affinity between entangled heteropeptide aggregates and the gold surface than the homopeptide case.

Nevertheless the present findings reveal a decrease of physisorption for the NGF(1-14)–BDNF(1-12) which can be ascribed to the considerable electrostatic forces occurring between the two peptides which shield the interaction with the Au_2O_3.

Based on the experimental data evidence, one can conclude that the growth onto Au_2O_3 takes place with the coverage by means of not-coupled (single) peptide molecules, which form a first, irreversibly physisorbed layer onto the surface. The peptide adlayer growth on the gold surface is due to the further deposition of weakly bound molecules onto such a first adlayer.

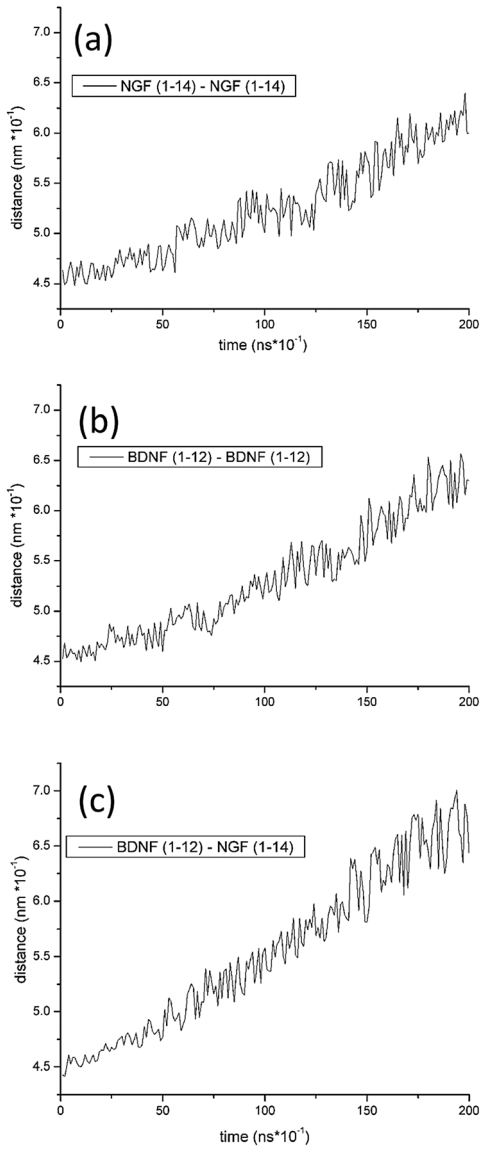

Fig. 6 Fluctuation of the peptide–Au_2O_3 distance over time calculated for: (a) NGF(1-14)–NGF(1-14) homodimer; (b) BDNF(1-12)–BDNF(1-12) homodimer; and (c) NGF(1-14)–BDNF(1-12) heterodimer.

4.4. NGF(1-14) and BDNF(1-12) adlayers interaction with neuroblastoma cells

Preliminary biological measurements on the viability of SH-SY5Y neuroblastoma cells showed that NGF(1-14) and BDNF(1-12) peptides adsorbed on the gold surfaces maintain a certain biological activity, thus demonstrating the positive response of the prepared substrates as adhesive and non-toxic supports for the used cells.

Promisingly, the cell viability assessed by the MTT test (Fig. 7) reveals that all the Au-covered surfaces are highly biocompatible, allowing SH-SY5Y neuroblastoma cells to grow better than on the control cell culture Petri dish surfaces.

It is to be noted that the highest viability is found on the bare gold substrates. This fact is not surprising because of the known properties of gold as noncytotoxic, nonimmunogenic, and biocompatible material.[28,29] In particular, the Lewis base character of the substrates (see ESI†), among other relevant physicochemical surface parameters, including charge,[30,31] topography[32,33] and specific chemical moieties[34,35] is pivotal in triggering the adsorption of proteins present in the medium onto the material

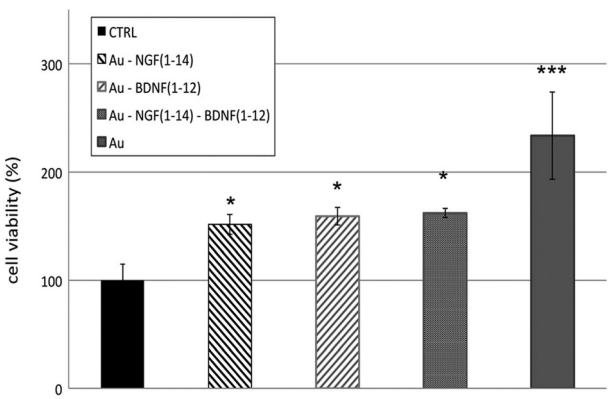

Fig. 7 Viability data from MTT assay of SH-SY5Y cells adhered on the different peptides immobilized on the gold surfaces. Data are normalized with respect to the control Petri dish substrate. (*$p < 0.05$; ***$p < 0.001$ *vs.* control).

surface in the early moments of cell contact with them.[18,36] This process, in turn, mediates the subsequent cellular events such as adhesion, proliferation, and differentiation.[37]

Intriguingly, the MTT test reveals that the neuronal vitality after interaction with NGF(1-14)– and BDNF(1-12)–gold substrates is higher compared to the control, in agreement with previously reported results on the proliferative activity of such peptides supplemented to the cells in the culture medium.[7,8]

Moreover, the cellular vitality on the substrates where the peptides adsorbed from the binary NGF(1-14) + BDNF(1-12) solution is comparable to that observed on the gold platforms where the peptides were adsorbed from single NGF(1-14) or BDNF(1-12) solution. By comparison with QCM-D and CD results discussed in Section 4.2, this finding can be taken as a further indirect proof of the competitive and functional interaction of the two peptides within the surface. That is, the cellular response to the NGF(1-14) and BDNF(1-12) peptide fragments immobilized on the gold surfaces is not a direct consequence of the corresponding areal mass coverage, but is affected by a more complex scenario, where the specific peptide–surface and peptide–peptide interactions, and the consequent viscoelastic properties of the hydrodynamic adlayer, modulate the overall behaviour at the biointerface.

In this respect, a possible synergic activity of NGF(1-14) and BDNF(1-12) peptides in the heterodimer adsorbed on the gold surface might be invoked. Further ongoing experiments aim to unravel this aspect.

Therefore, other than the development of strategies in peptide design, chemistry and assembly, an effort is necessary to design and scrutinize the response of peptide-mimicking materials exhibiting complexity, coordinated molecular processes, and dynamic interactions with the cells.[36]

5. Conclusions

In summary, we addressed here the immobilization of NGF(1-14) and BDNF(1-12) peptides on gold surfaces by a simple approach of spontaneous irreversible physical adsorption.

Experimental findings by QCM-D and CD analyses, as well as theoretical MD calculations, highlight the different interactions between each peptide and the gold surface, which affect, in turn, hydrodynamic thickness and related viscoelastic properties of the adlayer. Moreover, the differences found under the two different pH conditions investigated, suggest the possibility of fine tuning and triggering of the viscoelastic properties of the peptide adlayers, including shear modulus, viscosity, effective thickness and water content.

In particular, a synergic play of the two peptides in the adsorption on the gold is found at physiological pH, mostly related to the strong interaction between NGF(1-14) and BDNF(1-12) molecules in the bulk solution, whereas a predominance of BDNF(1-12) in the adlayer is highlighted at the acid pH of 5.5, thus indicating a competitive peptide adsorption process under these conditions. Preliminary cellular assays demonstrated the maintenance of biological properties of the peptides adsorbed on gold with respect to the bulk solution behaviour. Biochemical assays are currently in progress to figure out if NGF(1-14) and BDNF(1-12) immobilized on the gold surface can exert their independent action, binding and activating their cognate Trk receptors, or if the interaction with the gold surface affects/modulates their signaling cascades.

The presented results are promising for the implementation of the proposed approach and systems to nanoparticles loaded with the neurotrophin-mimicking peptides, able to maintain their biological properties and pH-triggered loading and drug release processes.

Acknowledgements

D. LM. acknowledges the MIUR (Italian Ministry for Research and University) grant PRIN 2010 (2010M2JARJ).

Notes and references

1 K. Saha, S. S. Agasti, C. Kim, X. Li and V. M. Rotello, *Chem. Rev.*, 2012, **112**, 2739.
2 M. Hnilova, E. E. Oren, U. O. S. Seker, B. R. Wilson, S. Collino, J. S. Evans, C. Tamerler and M. Sarikaya, *Langmuir*, 2008, **24**, 12440.
3 A. Vila Verde, J. M. Acres and J. K. Maranas, *Biomacromolecules*, 2009, **10**, 2118.
4 C. Satriano, M. E. Fragalà, G. Forte, A. M. Santoro, D. La Mendola and B. Kasemo, *Soft Matter*, 2012, **8**, 53.
5 C. Satriano, S. Svedhem and B. Kasemo, *Phys. Chem. Chem. Phys.*, 2012, **14**, 16695.
6 A. Travaglia, C. Satriano, M. L. Giuffrida, D. La Mendola, E. Rampazzo, L. Prodi and E. Rizzarelli, *Soft Matter*, 2013, **9**, 4648.
7 A. Travaglia, G. Arena, R. Fattorusso, C. Isernia, D. La Mendola, G. Malgieri, V. G. Nicoletti and E. Rizzarelli, *Chem.–Eur. J.*, 2011, **17**, 3726.
8 A. Travaglia, D. La Mendola, A. Magrì, V. G. Nicoletti, A. Pietropaolo and E. Rizzarelli, *Chem.–Eur. J.*, 2012, **18**, 15618.
9 R. Levi-Montalcini, *Science*, 1987, **237**, 1154.
10 A. M. Lohof, N. Y. Ip and M. M. Poo, *Nature*, 1993, **363**, 350.
11 H. Kang and E. M. Schuman, *Science*, 1995, **267**, 1658.
12 A. Travaglia, A. Pietropaolo, D. La Mendola, V. G. Nicoletti and E. Rizzarelli, *J. Inorg. Biochem.*, 2011, **111**, 130.
13 A. Schramm, J. H. Schulte, K. Astrahantseff, O. Apostolov, V. Limpt, H. Sieverts, S. Kuhfittig-Kulle, P. Pfeiffer, R. Versteeg and A. Eggert, *Cancer Lett.*, 2005, **228**, 143.
14 A. Cattaneo, S. Capsoni and F. Paoletti, *J. Alzheimer's Dis.*, 2008, **15**, 255.
15 L. Calorini, S. Peppicelli and F. Bianchini, *Exp. Oncol.*, 2012, **34**, 79.
16 G. J. del Zoppo, *Ann. N. Y. Acad. Sci.*, 2012, **1268**, 127.
17 D. Y. Kowk and A. W. Neumann, *Adv. Colloid Interface Sci.*, 1999, **81**, 16.
18 C. Satriano, S. Carnazza, A. Licciardello, S. Guglielmino and G. Marletta, *J. Vac. Sci. Technol., A*, 2003, **21**, 1145.

19 G. Sauerbrey, *Z. Phys.*, 1959, **155**, 206.
20 M. Rodahl, F. Höök, C. Fredriksson, C. A. Keller, A. Krozer, P. Brzezinski, M. Voinova and B. Kasemo, *Faraday Discuss.*, 1997, **107**, 229.
21 F. Höök, M. Rodahl, B. Kasemo and P. Brzezinski, *Proc. Natl. Acad. Sci. U. S. A.*, 1998, **95**, 12271.
22 M. V. Voinova, M. Rodahl, M. Jonson and B. Kasemo, *Phys. Scr*, 1999, **59**, 391.
23 P. Dauber-Osguthorpe, V. A. Roberts, D. J. Osguthorpe, J. Wolff, M. Genest and A. T. Hagler, *Proteins: Struct., Funct., Genet.*, 1988, **4**, 31.
24 K. F. Lau, H. E. Alper, T. S. Thacher and T. R. Stouch, *J. Phys. Chem.*, 1994, **98**, 8785.
25 H. J. C. Berendsen, J. P. M. Postma, W. F. van Gunsteren, A. Di Nola and J. R. Haak, *J. Chem. Phys.*, 1984, **81**, 3684.
26 P. G. Jones, H. Rumpel, E. Schwarzmann, G. M. Sheldrick and H. Paulus, *Acta Crystallogr., Sect. B: Struct. Crystallogr. Cryst. Chem.*, 1979, **35**, 1435.
27 R. F. Tabor, A. J. Morfa, F. Grieser, D. Y. C. Chan and R. R. Dagastine, *Langmuir*, 2011, **27**, 6026.
28 R. Shukla, V. Bansal, M. Chaudhary, A. Basu, R. R. Bhonde and M. Sastry, *Langmuir*, 2005, **21**, 10644.
29 V. Brunetti, G. Maiorano, L. Rizzello, B. Sorce, S. Sabella, R. Cingolani and P. P. Pompa, *Proc. Natl. Acad. Sci. U. S. A.*, 2010, **107**, 6264.
30 B. Joddar and Y. Ito, *J. Mater. Chem.*, 2011, **21**, 13737.
31 Y. Xu, M. Takai and K. Ishihara, *Biomaterials*, 2009, **30**, 4930.
32 C. Satriano and M. E. Fragalà, *RSC Adv.*, 2012, **2**, 3607.
33 E. M. Frohlich, X. Zhang and J. L. Charest, *Integr. Biol.*, 2012, **4**, 75.
34 J. Robertus, W. R. Browne and B. L. Feringa, *Chem. Soc. Rev.*, 2010, **39**, 354.
35 L. Perlin, S. MacNeil and S. Rimmer, *Soft Matter*, 2008, **4**, 2331.
36 C. Satriano, G. M. L. Messina, S. Carnazza, S. Guglielmino and G. Marletta, *Mater. Sci. Eng., C*, 2006, **26**, 942.
37 J. H. Collier and T. Segura, *Biomaterials*, 2011, **32**, 4198.

